Hao Ling · Ahmed A. Shabana

# Euler angles and numerical representation of the railroad track geometry

**Abstract** The geometry description plays a central role in many engineering applications and directly influences the quality of the computer simulation results. The geometry of a space curve can be completely defined in terms of two parameters: the *horizontal* and *vertical curvatures*, or equivalently, the curve *curvature* and *torsion*. In this paper, distinction is made between the track angle and space-curve bank angle, referred to in this paper as the *Frenet bank angle*. In railroad vehicle systems, the *track bank angle* measures the track *super-elevation* required to define a *balance speed* and achieve a safe vehicle operation. The formulation of the track space-curve differential equations in terms of Euler angles, however, shows the dependence of the *Frenet bank angle* on two independent parameters, often used as inputs in the definition of the track geometry. This paper develops the general differential equations that govern the track geometry using the Euler angle sequence adopted in practice. It is shown by an example that a curve can be twisted and vertically elevated but not super-elevated while maintaining a constant *vertical-development angle*. The continuity conditions at the track segment transitions are also examined. As discussed in the paper, imposing curvature continuity does not ensure continuity of the tangent vectors at the curve/spiral intersection. Several curve geometries that include planar and helix curves are used to explain some of the fundamental issues addressed in this study.

## 1 Introduction

In railroad vehicle system dynamics, the description of the track geometry enters into the formulation of the wheel/rail contact problem. Therefore, a proper numerical representation of the track geometry is necessary in order to accurately define the locations of the contact points and predict correctly the wheel/rail contact forces [1–20]. The track geometry is numerically described using a point mesh that defines the location of material points on the track centerline and rail space curves. At each nodal point, specific data are provided in order to define the point locations as well as rotation coordinates that define the curve geometry as well as the track frames that follow the vehicle components in railroad vehicle formulations. These data include the space-curve arc length parameter that corresponds to the node, the coordinates of the position vector of the node, and three Euler angles that define the track geometry and the orientation of the track frames. Having the position and angle nodal information, an interpolation scheme is used during the dynamic simulation in order to determine the geometry at a contact point within a track segment. In order to achieve the desired accuracy, the lengths of the segments in the track geometry file are chosen small, and therefore, this track geometry file, often created in a preprocessor computer program, can be very large.

H. Ling · A. A. Shabana (✉)
Department of Mechanical and Industrial Engineering, University of Illinois at Chicago, 842 West Taylor Street, Chicago, IL 60607, USA
e-mail: shabana@uic.edu

H. Ling
e-mail: hling9@uic.edu

The track layout is normally constructed using three basic segments: *tangent*, *curve*, and *spiral*. The tangent segment is straight and has zero curvature; the curve segment has a constant curvature; and the spiral segment that connects two segments with varying curvatures is designed to have a linearly varying curvature. In the case of a curve segment, use of super-elevation is necessary in order to create a gravity force component that balances the centrifugal force when the vehicle negotiates the curve. Therefore, tracks are curved horizontally, elevated vertically, and super-elevated in the case of curved segments. While the spiral segments are introduced to reduce the possibility of derailments, accidents still occur when trains negotiate the spiral sections of the track because of inappropriate designs resulting from lack of good understanding of their geometry. Consequently, understanding the spiral geometry, particularly at the transition points which define the intersections of segments with different geometries, is necessary in order to avoid deadly, costly, and environmentally damaging accidents. Virtual prototyping and computer simulations can play a significant role in understanding the cause of these accidents.

In order to develop the numerical representation of the track geometry and determine the position coordinates and angles at the nodal points in a preprocessor computer program, three pieces of information, at each track point at which the geometry changes, are provided. These pieces of information are the *horizontal curvature*, *grade*, and *track bank angle*. Because a track can have very long straight and curved segments, the input to the preprocessor computer program that produces the track geometry file is simple, despite the fact that the output of this preprocessor can be a very large file in which the nodal position coordinates and Euler angles are provided. The three inputs to the preprocessor computer program are used in the numerical construction of the track geometry and are associated with three Euler angles: the *horizontal-curvature angle* $\psi$, the *vertical-development angle* $\theta$, and the *track bank angle* $\phi_t$, defined using the Euler sequence $Z, -Y$, and $-X$, where $X$ is the longitudinal axis, $Y$ is the lateral axis, and $Z$ is the vertical axis [18, 19]. These three angles serve to completely define the track geometry, and therefore, they are used as geometric parameters. The negative signs for the axes $Y$ and $X$ are used for consistency with practical considerations used in the layout of the track structure.

The three Euler angles $\psi$, $\theta$, and $\phi_t$ are treated in existing railroad vehicle algorithms as independent geometric parameters. Nonetheless, as it has been demonstrated recently, Euler angles used in the general description of curve geometry are not totally independent because the geometry of a space curve is completely defined using two independent geometric parameters only [21, 22]. In existing railroad algorithms, the curvature angle $\psi$ is determined using the horizontal curvature $C_H$, which is the first input to the track preprocessor; and the vertical development angle $\theta$ is determined using the second input which is the vertical curvature $C_V$. The track bank angle $\phi_t$ is determined from the third input which defines the super-elevation. Assuming that the track bank angle is independent, linear interpolation is used to convert it to a field variable within a track segment. In this linear interpolation, the two bank angles at the two ends of a segment are used. Nonetheless, the use of this approach, which is based on providing three inputs, implies that these three Euler angles are independent, and such an assumption is justified when defining the orientation of the track frames that follow the vehicle components. However, because the geometry of a space curve is completely defined using two variables [23, 24], the track bank angle $\phi_t$ obtained using the independent linear interpolation is not the Frenet bank angle $\phi$ used in the definition of the geometry of the space curve. The direction of the *centrifugal force* is defined by the bank angle of the motion trajectory curve and not by the track bank angle obtained using the linear interpolation. This distinction between the two bank angles (track and curve) is necessary in order to have a better understanding of the track geometry that has a significant effect on the vehicle dynamics and stability [25–29]. In this paper, a *field variable* refers to a variable that is a function of other parameters and has a continuous domain with infinite number of points, but with finite length. On the other hand, the phrase "*rigid rotation*" is used to refer to a rigid-body rotation of the curve that does not change the curve geometry, that is, a rigid rotation is a rigid-body rotation of the entire curve.

## 2 Scope and contributions of this investigation

The main objective of this investigation is to develop the general differential geometry equations of railroad tracks in terms of the Euler angle sequence used in practice. This Section explains the scope and the specific contributions of this study.

## 2.1 Scope of this investigation

As previously mentioned, in the virtual prototyping of railroad vehicle systems, a track preprocessor is often used to define the geometry of the track centerline curve and the right and left rail space curves. For each curve, the large point mesh data are generated by the track preprocessor based on the values of the horizontal curvature, grade, and super-elevation provided at few points at which the track geometry changes. These data define the positions and the orientation of track frames at a large number of nodal points. These points are normally spaced one feet apart in order to ensure the accuracy of the interpolation during the dynamic simulations. At each node, three Euler angles are provided in order to define the orientation of the track frames at the nodes, and such a description is justified because the orientation of a coordinate system in space can be defined using three independent angles.

Nonetheless, it is important to distinguish between the angles used to define the rail space curve geometry and the angles used to define the orientation of the track frames at the nodal points. In railroad vehicle algorithms, both sets of angles share two angles, the horizontal curvature angle $\psi$ and the vertical development angle $\theta$. In the case of the track frames, the third angle is the *track bank angle* $\phi_t$ used to define the track super-elevation used in the computation of the balance speed. This track bank angle $\phi_t$ is defined at the nodes using independent linear interpolation. While this angle is used to define the balance speed and determine the component of the gravity force that balances the lateral component of the centrifugal force, such a track bank angle is not the angle that defines the direction of the centrifugal force, which is often assumed parallel to the horizontal plane when the balance speed is determined. The track frames, whose orientations are defined using the three independent Euler angles $\psi$, $\theta$, and $\phi_t$ at the track nodes, follow the motion of the vehicle components and are used in the formulation of kinematic equations of railroad vehicle systems. The linear interpolation used for the track bank angle $\phi_t$ defines the super-elevation of the track in the transition sections.

The geometry of the track centerline curve and right and left rail space curves can also be described using three Euler angles. However, these three Euler angles for a space curve are not totally independent because the curve geometry can be described in terms of only two independent geometric parameters [21, 22]. Therefore, a distinction must be made between Euler angles used in the definition of the track frames that follow the motion of the vehicle components and Euler angles that define the geometry of the space curves. In railroad vehicle dynamics algorithms, the track frames and the space curves share the two angles $\psi$ and $\theta$, but differ by one rotation. The third rotation used to define the space curve geometry is the *curve bank angle* $\phi$, referred to in this paper as the *Frenet bank angle*, which can be obtained from the two angles $\psi$ and $\theta$ using an algebraic equation, as demonstrated in this study. It is important, however, to distinguish between the two angles $\phi_t$ and $\phi$ in order to shed light on the linear interpolation used to determine $\phi_t$ which does not enter into the definition of the curve geometry, does not directly define the direction of the centrifugal force, and is used mainly to define the track super-elevation and the balance speed. This investigation is focused on developing the general differential geometry equations of the rail space curves in order to have a better understanding of the fundamental difference between the track and Frenet bank angles. This understanding will allow addressing geometry, design, and discontinuity problems at the track transitions which will be the subject of future investigations.

## 2.2 Contributions of this investigation

The specific contributions of this study are summarized as follows:

1. The differential geometry equations of the track space curve are formulated in terms of the three Euler angles used by the rail industry: the horizontal curvature, vertical development, and Frenet bank angles. Using this angle representation, the matrix that defines the orientation of the Frenet frame along the space curve is formulated. The solution of the differential geometry equations developed in this study defines completely the angles.

2. The paper introduces the new definition of the *Frenet bank angle* to the railroad literature and demonstrates that the rail curve (spiral) bank angle can be determined from an algebraic equation in terms of two inputs, and consequently, the Frenet bank angle cannot be considered as a third independent parameter. This distinguishes this bank angle from the track bank angle which enters into the definition of the orientation of the track frames, is treated as an independent angle, and is linearly interpolated in the numerical description of the track geometry in railroad vehicle algorithms.

3. The differential equation singularity that results from a rigid rotation of a track segment is explained. The track segment geometry is invariant under a rigid rotation, and therefore, such a rigid rotation does not influence the differential geometry equations developed in this study. Another special case which is discussed in this paper is the case of constant horizontal and vertical curvatures, as in the case of a helix curve. The curve elevation and the vertical development angle and their relationship to the bank angle in this special case of constant curvature and torsion are discussed.
4. Using an example, the paper demonstrates that a curve can be twisted and vertically elevated, but not super-elevated while maintaining a constant vertical development angle which is not a rigid rotation. Using a helix curve, it is shown that the helix curvature vector remains in the horizontal plane, and the acceleration of a particle tracing the helix curve with a constant forward velocity has no vertical component. This result is consistent with the fact that a helix curve has zero Frenet bank angle. In this paper, the phrase "*super-elevated curve*" is used to indicate that the curve has nonzero Frenet bank angle.
5. The paper examines the degree of continuity at the intersection of two track segments with different geometries. It is shown that position and curvature continuities do not ensure smoothness because of the discontinuity in the tangent vectors. The results obtained using the curvature continuity conditions are compared with the results obtained by imposing slope continuity.

## 3 Track differential geometry equations

The use of Euler angles in the definition of the track curve geometry leads to three equations in a differential form. Two of these equations define the curvature and torsion of the space curve in terms of Euler angles and their derivatives [21, 22]. If the curve curvature and torsion are given, these three differential equations can be integrated numerically to define Euler angles as functions of the curve arc length, demonstrating that the three Euler angles of a space curve are not independent. In this Section, the sequence of Euler angles adopted in practice in the numerical definition of the track geometry is used.

### 3.1 Euler angle representation of space curves

In the description of the track geometry, Euler angles are used as geometric variables and not motion variables. Using a track coordinate system $X^r Y^r Z^r$, the track space-curve geometry can be described using the three Euler angles $\psi$, $\theta$, and $\phi$ about the axes $Z^r$, $-Y^r$, and $-X^r$, respectively. This sequence is used because of practical considerations, as previously discussed [18, 19]. These three Euler angles are related, respectively, to the horizontal curvature, grade, and super-elevation, used by the rail industry as inputs to define numerically the track geometry. The orientation of a coordinate system at an arbitrary point on the track space curve can be defined in terms of these three Euler angles as

$$\mathbf{A} = \begin{bmatrix} \cos\psi\cos\theta & -\sin\psi\cos\phi + \cos\psi\sin\theta\sin\phi & -\sin\psi\sin\phi - \cos\psi\sin\theta\cos\phi \\ \sin\psi\cos\theta & \cos\psi\cos\phi + \sin\psi\sin\theta\sin\phi & \cos\psi\sin\phi - \sin\psi\sin\theta\cos\phi \\ \sin\theta & -\cos\theta\sin\phi & \cos\theta\cos\phi \end{bmatrix}. \quad (1)$$

If certain relationships are established between Euler angles, the above matrix can be used to define the Frenet frame at an arbitrary point on the space curve. Following the systematic procedure described in a recent publication, one can show that [22]

$$\begin{bmatrix} \tau \\ 0 \\ \kappa \end{bmatrix} = \bar{\mathbf{G}}\left(\frac{\partial\boldsymbol{\theta}}{\partial s}\right) = \begin{bmatrix} \psi'\sin\theta - \phi' \\ -\psi'\sin\phi\cos\theta - \theta'\cos\phi \\ \psi'\cos\phi\cos\theta - \theta'\sin\phi \end{bmatrix} \quad (2)$$

where $\kappa$ and $\tau$ are, respectively, the curvature and torsion of the track space curve, $\boldsymbol{\theta} = \begin{bmatrix} \psi & \theta & \phi \end{bmatrix}^T$, $s$ is the arc length, $a' = \partial a / \partial s$, and the columns of the matrix $\bar{\mathbf{G}}$ define the three axes, in the coordinate system $X^r Y^r Z^r$, about which the three Euler rotations are performed, that is,

$$\bar{\mathbf{G}} = \begin{bmatrix} \sin\theta & 0 & -1 \\ -\sin\phi\cos\theta & -\cos\phi & 0 \\ \cos\phi\cos\theta & -\sin\phi & 0 \end{bmatrix}. \quad (3)$$

Equation (2) defines the curvature and torsion in terms of Euler angles and their derivatives as

$$\left.\begin{aligned} \kappa &= \psi' \cos\phi \cos\theta - \theta' \sin\phi \\ \tau &= \psi' \sin\theta - \phi' \end{aligned}\right\}. \tag{4}$$

It is clear from this equation that the curve torsion can be nonzero even in the case of constant angle $\phi$. Using Eq. (2), one can show that the derivatives of Euler angles can be written in terms of the curvature and torsion as

$$\left.\begin{aligned} \psi' &= \kappa \cos\phi \big/ \cos\theta \\ \theta' &= -\kappa \sin\phi \\ \phi' &= \kappa \tan\theta \cos\phi - \tau \end{aligned}\right\}. \tag{5}$$

The preceding equations demonstrate that if the curvature and torsion of the curve are given, the three Euler angles can be determined using numerical integration. That is, the three Euler angles can be written in terms of only two parameters, and therefore, these three angles for a space curve are not totally independent as will be further explained in later Sections of this paper.

Distinction is made between the curve (Frenet) and track bank angles $\phi$ and $\phi_t$, respectively, as previously mentioned. One can think of the super-elevation as the result of the bank angle $\phi_t$ as the orientation of the ties (sleepers). That is, the track bank angle $\phi_t$ defines the track super-elevation (tie orientation), while the Frenet bank angle $\phi$ that enters into the definition of the curve geometry is independent of the orientation of the tie or the track plane. It is important to also note that the rail can be canted inward, and such a canting has an effect on the rail vehicle dynamics and the wheel/rail contact forces. The track bank angle $\phi_t$ is used in the computer simulations to define the orientation of the track frames that serve as a reference to and follow the vehicle components. This is the angle that is linearly interpolated in the railroad algorithms and not the Frenet bank angle $\phi$ that enters into the definition of the curve geometry.

### 3.2 Differential singularity

It is clear from Eq. (3) that the matrix $\bar{\mathbf{G}}$ is singular if $\theta = \pi/2$. If $\theta$ is constant, different from zero, and describes a rigid rotation, one has from the second relation in Eq. (2), $\psi' \sin\phi \cos\theta = 0$. Since in a general rigid rotation $\cos\theta \neq 0$ and since a planar curve with an arbitrary curvature is invariant under a rigid body rotation, the equation $\psi' \sin\phi \cos\theta = 0$ implies that $\phi = 0$. For such a singular configuration, the differential relationships of Eq. (5) no longer hold.

In this paper, distinction is made between rigid and constant rotations; a rigid rotation is a special case of a constant rotation. While a rigid rotation is a constant rotation within the track segment and does not depend on the arc length parameter, such a rigid rotation does not contribute to a change in the curve geometry. Nonetheless, not every constant rotation is considered a rigid rotation. While the geometry of a curve is invariant under an arbitrary rigid rotation, as explained using the helix curve example, a curve can have zero vertical curvature $C_V$ and nonzero torsion $\tau$ because the vertical development angle $\theta$ defined by the relationship $\mathrm{d}\theta/\mathrm{d}s = C_V$ is different from zero and is a constant rotation.

### 3.3 Use of Frenet frame

Because the three Euler angles used in the definition of the curve geometry are not independent, Eq. (1) defines the orientation of the Frenet frame at points on the curve defined by the arc length $s$ [21, 22]. While the Frenet frame is used in this study, the sequence of Euler angles used by the rail engineers to define the numerical description of the track geometry can always be related to and associated with any other representation of the track frame. The advantage of using the Euler angle sequence with the Frenet frame, however, is to have a direct relationship between the angles and the geometric invariants of a curve such as the curvature and torsion. Furthermore, the centrifugal inertia force that arises during curve negotiations is in the direction of the curvature vector that represents one of the axes of the Frenet frame. If the curve is defined in its parametric form by the equations $\mathbf{r} = \mathbf{r}(s)$, where $s$ is the arc length, the velocity vector is defined along the vector tangent to the curve as $\dot{\mathbf{r}} = \dot{s}\mathbf{r}_s$, where $\mathbf{r}_s = \partial\mathbf{r}/\partial s$ is the unit tangent. The acceleration vector is defined as $\ddot{\mathbf{r}} = (\dot{s})^2 \mathbf{r}_{ss} + \ddot{s}\mathbf{r}_s = \big((\dot{s})^2/R\big)\mathbf{n} + \ddot{s}\mathbf{r}_s$, where $\mathbf{n}$ is the unit normal and $R$ is the radius of curvature. Therefore, there

is a clear advantage in establishing the relationship between the axes of the Frenet frame and the Euler angle sequence used by the rail industry to define the track geometry. This is with the understanding that the bank angle of the motion trajectory curve defines the direction of the curve curvature vector and centrifugal force and not the linearly interpolated track bank angle $\phi_t$ that defines the track super-elevation. If the Frenet bank angle $\phi$ is zero, the curvature and centrifugal force vectors always lie in a plane parallel to the horizontal plane regardless of the value of the track bank angle $\phi_t$.

## 4 Numerical representation of the track geometry

The geometry of the track is defined in practice using three inputs at points of intersections of track segments with different geometries. Using these three inputs at few discrete points, a numerical representation of long tracks stretching hundreds of miles can be developed using a small set of data points. The values at the discrete points are used as end conditions that define corresponding field variables, considered in existing algorithms as independent to determine the track frames. Two different, but related, arc length parameters are often used in these algorithms: the space curve arc length parameter $s$ and the arc length $S$ of a curve defined by projecting the space curve on the horizontal plane.

### 4.1 Track inputs

The track inputs, assumed independent and provided at points of intersection of track segments with different geometric properties, are the following [18, 19]:

1. Horizontal curvature $C_H$: Input values of the horizontal curvature at endpoints of the track segments are used to define $C_H$ as field variable function of the projected arc length $S$, that is, $C_H = C_H(S)$.
2. Vertical development angle $\theta$: Input values of the vertical development angle $\theta$ at endpoints of the track segments are used to define $\theta$ as field variable within the segment. In this case $\theta$ is written as function of the arc length parameter $s$ using the ratio of vertical and longitudinal distances, that is, $\theta = \theta(s)$.
3. Track bank angle $\phi_t$: Values of the track bank angle, which describes the super-elevation, at endpoints of the segments are used to write $\phi_t$ as field variable function of the projected arc length $S$, that is, $\phi_t = \phi_t(S)$.

These three track geometry inputs are treated in existing algorithms as independent and unrelated, as previously discussed.

### 4.2 Horizontal curvature

The *horizontal curvature* is the curvature of the curve obtained by projecting the track space curve on the horizontal plane. Therefore, one has $dS = \cos\theta\,ds$, where $S$ is the arc length of the projected curve and $s$ is the arc length of the track space curve. For a spiral segment, the horizontal curvature is assumed to vary linearly between two endpoints. The horizontal curvature angle $\psi$ is obtained by the integration of $C_H(S)$ with respect to the projected arc length $S$ as $\psi(S) = \int_{s_0}^{s} C_H(S)\,dS$. Given the values of $C_H$ at the endpoints $S_0$ and $S_1$, and assuming that $C_H$ varies linearly within the segment, the equation $\psi(S) = \int_{s_0}^{s} C_H(S)\,dS$ can be used to determine the curvature angle $\psi$ at arbitrary discrete nodal points.

### 4.3 Vertical development angle

Given the grade at the endpoints of a segment, the vertical development angle $\theta$ can be defined from the ratio between the vertical and longitudinal distances within the track segment. The track segment is designed such that $d\theta/ds$ is constant, that is, $\theta(s) = (1 - \xi_d)\theta_0 + \xi_d\theta_1$, where $\theta_0 = \theta(s_0)$, $\theta_1 = \theta(s_1)$, and $\xi_d = s/(s_1 - s_0)$. The relationship between this angle and the vertical curvature $C_V$ of the space curve will be explained. It will be also shown that the formula $\theta(s) = (1 - \xi_d)\theta_0 + \xi_d\theta_1$ is the result of a numerical integration, and therefore, no linear interpolation assumptions are made in this case.

### 4.4 Track bank angle

Given the values of the super-elevation at the endpoints of a segment, the track bank angle $\phi_t$, used to define the orientation of the track frame, can be defined as a field variable within the segment using a linear interpolation with respect to the arc length $S$, that is, $\phi_t = \phi_t(S)$. This linear interpolation implies that the track bank angle $\phi_t$ is independent of the horizontal curvature angle $\psi$ and the vertical development angle $\theta$. This is one of the important issues addressed in this investigation since distinction needs to be made between the independent track bank angle $\phi_t$ obtained using the linear interpolation to define the orientations of the track frames, and the Frenet bank angle $\phi$ that enters directly into the definition of the curve geometry and defines the direction of the centrifugal force if a mass traces this curve.

### 4.5 Transition continuity

In the numerical description of the track, the continuity conditions at the track transitions are defined using algebraic equations. Therefore, the degree of continuity depends on the number of algebraic equations imposed to achieve a certain level of smoothness. Continuity of higher derivatives does not always imply continuity of lower derivatives. For example, two separate and disconnected curves can have the same gradients and curvatures, but not the same coordinates. One can also have two separate and disconnected curves and use one algebraic equation to impose a condition that the curvatures of the two curves at a point are the same. Such an algebraic equation does not guarantee continuity of the position or gradients at the two points. Therefore, imposing continuity of three track geometric variables does not necessarily imply continuity of other geometric variables including the gradients whose continuity is desirable in order to achieve smoothness at the track transitions in the numerical representation of the track geometry. While in practice smoothing adjustments are often made, the numerical representation of the track is based on only three measurements: the horizontal curvature, the grade, and the super-elevation. These three measurements are sufficient to determine Euler angles used to define the track geometry in the computer simulations, but are not sufficient to ensure the gradient continuity. After determining Euler angles at the nodal points of the track in a track preprocessor computer program, gradient continuity can be ensured by using the angles to determine gradient vectors to be used with the interpolation of the absolute nodal coordinate formulation (ANCF) as discussed in the literature.

## 5 Bank angle and curve geometry

Using the space-curve equations presented in Sect. 3, one can demonstrate that the procedures used for converting the horizontal curvature angle $\psi$ and the vertical development angle $\theta$ to field variables are consistent with the differential geometry analysis.

### 5.1 Curvature vector

In order to better understand the procedures used in practice and their relationship to the differential geometry theory of curves, the unit tangent vector which is the first column of the transformation matrix of Eq. (1) is differentiated with respect to the arc length $s$ in order to define the curvature vector $\mathbf{K}$ using the Euler angle sequence used in practice. This leads to

$$\mathbf{K} = \begin{bmatrix} -\psi' \sin\psi \cos\theta - \theta' \cos\psi \sin\theta \\ \psi' \cos\psi \cos\theta - \theta' \sin\psi \sin\theta \\ \theta' \cos\theta \end{bmatrix} = \psi' \begin{bmatrix} -\sin\psi \cos\theta \\ \cos\psi \cos\theta \\ 0 \end{bmatrix} + \theta' \begin{bmatrix} -\cos\psi \sin\theta \\ -\sin\psi \sin\theta \\ \cos\theta \end{bmatrix}. \qquad (6)$$

This equation shows that the curvature vector has two components $\psi' = \partial\psi / \partial s$ along the unit vector $\mathbf{v}_1 = \begin{bmatrix} -\sin\psi \cos\theta & \cos\psi \cos\theta & 0 \end{bmatrix}^T$ defined in the horizontal plane, and $\theta' = \partial\theta / \partial s$ along the unit vector $\mathbf{v}_2 = \begin{bmatrix} -\cos\psi \sin\theta & -\sin\psi \sin\theta & \cos\theta \end{bmatrix}^T$ which is perpendicular to the track plane before performing the last Euler rotation $\phi$. For example, if $\phi$ is equal to zero in Eq. (1), $\mathbf{v}_2$ represents the third column of the transformation matrix $\mathbf{A}$ and defines a unit vector along the $Z^r$ axis of the track coordinate system. It is clear that the two vectors $\mathbf{v}_1$ and $\mathbf{v}_2$ are orthogonal unit vectors. It can be shown that the curvature vector of Eq. (6) is

parallel to the vector that defines the second column of the transformation matrix $\mathbf{A}$ of Eq. (1) [21, 22]. Using Eq. (6), one can define the horizontal curvature $C_H$ and vertical curvature $C_V$ as

$$\left.\begin{aligned} C_H &= \frac{\partial \psi}{\partial S} = \frac{\partial \psi}{\partial s}\frac{\partial s}{\partial S} = \frac{\psi'}{\cos \theta} \\ C_V &= \frac{\partial \theta}{\partial s} = \theta' \end{aligned}\right\}. \tag{7}$$

This equation shows that the procedure used in practice for determining the horizontal curvature angle $\psi$ from $C_H$ is consistent with the differential geometry theory of curves. In practice, track segments are designed such that the horizontal curvature $C_H$ varies linearly. Therefore, no interpolation assumptions are made in converting $\psi$ to a geometric field variable.

The second equation in Eq. (7), on the other hand, shows that $\mathrm{d}\theta / \mathrm{d}s = C_V$, which leads to $\theta(s) = \theta(s_0) + \int_{s_0}^{s_1} C_V \mathrm{d}s$. Track segments are designed to have a constant vertical curvature $C_V$, and therefore, one has $C_V = (\theta(s) - \theta(s_0)) / (s - s_0)$. This equation is not the result of a linear interpolation assumption; it is the result of numerical integration based on a design consideration of the track segment.

In summary, the procedure used for converting the horizontal curvature angle $\psi$ and the vertical development angle $\theta$ to field variables is consistent with the differential geometry theory of curves and does not involve any assumptions of linear interpolation. This fact is important in the discussion and analysis presented in the remainder of this paper.

## 5.2 Torsion and vertical curvature

While a space curve is uniquely defined by its curvature and torsion, one can show that the torsion (twist) can be replaced by the vertical curvature used in the railroad algorithms. That is, a curve is uniquely defined by its horizontal and vertical curvatures. In order to demonstrate that the curve can be uniquely defined in terms of $C_H$ and $C_V$, the first and second equations in Eq. (5) are written as

$$\left.\begin{aligned} \psi' &= C_H \cos \theta = \kappa \cos \phi / \cos \theta \\ \theta' &= C_V = -\kappa \sin \phi \end{aligned}\right\}. \tag{8}$$

Using the expression of the curvature components, one can write

$$\kappa = \sqrt{\left(C_H \cos^2 \theta\right)^2 + C_V^2}. \tag{9}$$

The second equation in Eq. (2) can also be used to obtain an expression for the Frenet bank angle $\phi$ in terms of the derivatives of the two other Euler angles. This relationship can be used to write the torsion $\tau$ in terms of the derivatives of the two angles $\psi$ and $\theta$ defined in Eq. (8), demonstrating that the track space curve is uniquely defined by its horizontal and vertical curvatures.

## 5.3 Frenet and track bank angles

By distinguishing the Frenet bank angle $\phi$ from the track bank angle $\phi_t$ and using Eqs. (2) and (8), one can write the third angle $\phi$ in terms of $C_H$ and $C_V$, as $\tan \phi = -C_V / C_H \cos^2 \theta$, or alternatively,

$$\phi = \tan^{-1}\left(-C_V / C_H \cos^2 \theta\right). \tag{10}$$

Using the first equation in Eq. (2), one has

$$\tau = \psi' \sin \theta - \phi' = \frac{1}{2} C_H \sin 2\theta - \phi'. \tag{11}$$

The torsion of a curve is invariant under a rigid-body rotation. Therefore, a super-elevation by a constant rigid bank angle $\phi$ within a track segment does not change the curve geometry including the torsion. In this case of rigid super-elevation angle, $\phi' = 0$. Additionally, one can, in general, write the derivative of $\phi$ by differentiating Eq. (10) with respect to the arc length as

$$\phi' = \sin 2\phi\left(C_V \tan \theta - \left(C_{HS} / 2C_H\right) \cos \theta\right). \tag{12}$$

In this equation, $C_{HS} = \partial C_H / \partial S$. Because in the construction of the track geometry $C_H$ is assumed as a linear function of the horizontal arc length $S$, $C_{HS} = \partial C_H / \partial S$ is constant. Equation (10) clearly shows that the Frenet bank angle $\phi$ can be completely defined using the horizontal and vertical curvatures. Therefore, such an angle cannot be considered as a third independent variable. This is consistent with the general theory of differential geometry that states that a space curve is uniquely defined by two geometric invariants: the curvature and torsion. The track bank angle $\phi_t$ obtained by a linear interpolation within the spiral curve is used to determine the orientations of the track frames, and this angle is different from the Frenet bank angle $\phi$ used in the definition of the curve geometry.

## 5.4 Summary of the equations

The analysis presented in this Section demonstrates that the derivatives of Euler angles can be uniquely determined using the horizontal and vertical curvatures used in practice. It is important, however, to point out that zero vertical curvature $C_V$ does not always imply zero torsion $\tau$ as will be demonstrated in this paper using the helix curve example. As an alternate to Eq. (5), the derivatives of Euler angles can be expressed in terms of the horizontal and vertical curvatures as

$$\left. \begin{array}{ll} \psi' = C_H \cos\theta, & \theta' = C_V \\ \phi' = \dfrac{1}{2}\sin 2\phi \left( 2C_V \tan\theta - \dfrac{C_{HS}}{C_H}\cos\theta \right) \end{array} \right\}. \tag{13}$$

It is clear from this equation that the use of the track segment design assumptions of linear horizontal curvature and constant vertical curvature does not, in general, lead to a constant derivative of the angle $\phi$. In fact, according to Eq. (10), the angle $\phi$ can be defined in terms of $C_H$, $C_V$, and the angle $\theta$ by an algebraic equation. Therefore, the preceding equations can be reorganized and written as

$$\psi' = C_H \cos\theta, \quad \theta' = C_V, \quad \phi = \tan^{-1}\left(-C_V / C_H \cos^2\theta\right). \tag{14.1–3}$$

This equation demonstrates that the Frenet bank angle cannot be considered an independent parameter.

## 6 Vertical development and super-elevation

In this Section, it is demonstrated that a constant vertical development angle does not always correspond to a rigid rotation. It is also demonstrated that a curve can be twisted and vertically elevated while the Frenet bank angle remains zero. To this end, a helix curve geometry is considered. Before considering the helix example, the case of planar curves is discussed in order to explain some configurations relevant to the argument made in the remainder of this paper.

### 6.1 Planar curves

It is clear from Eq. (14.3) that the value of $\phi$ can be uniquely defined along the arc length using the nonlinear algebraic equation $\phi = \tan^{-1}\left(-C_V / C_H \cos^2\theta\right)$. If the vertical development angle $\theta$ is small, $\cos\theta \approx 1$, and $\phi$ is mostly dependent on the ratio of $C_V / C_H$. In this case, $C_V = d\theta / ds$ is also small. If $C_H$ is zero, there is no need for a super-elevation or definition of a balance speed. This geometric configuration covers a straight track segment or a segment bent vertically, $C_V \neq 0$. Both cases do not require using super-elevation to balance the effect of the centrifugal forces. If $C_V = 0$ and $\theta = 0$, one obtains again an untwisted planar curve, and in this case the bank angle $\phi = 0$ and the curve torsion $\tau$ is zero as it is clear from Eq. (11), $\tau = \psi' \sin\theta - \phi' = (1/2)C_H \sin 2\theta - \phi'$. Therefore, the geometry of a planar curve, defined by one curvature component only, $C_H$ or $C_V$, and zero vertical development angle is completely described by one angle that varies with the arc length parameter regardless of whether or not this planar curve is defined in the horizontal or vertical plane.
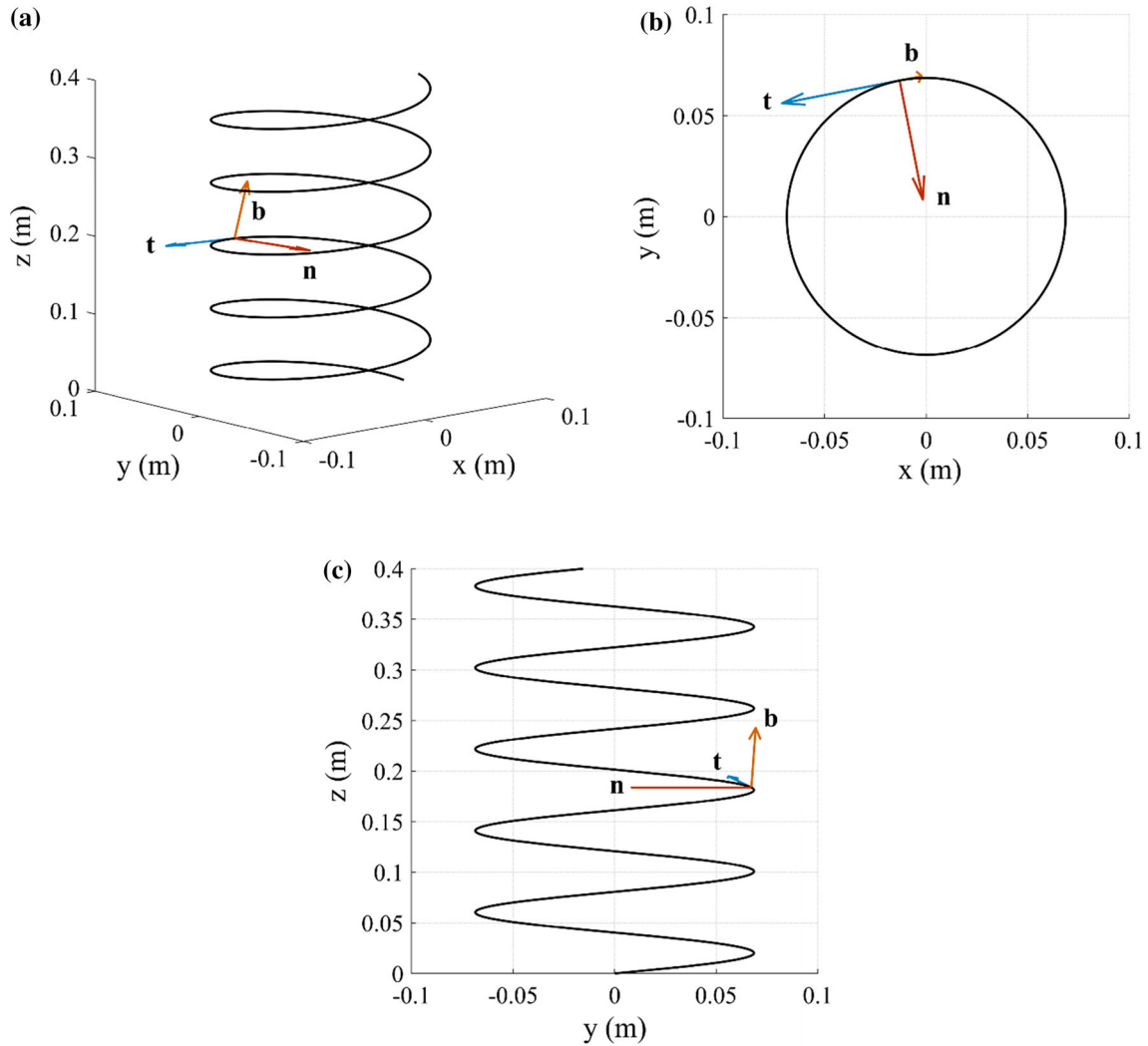
**(a)**



**(b)**



**(c)**



Fig. 1 Helix geometry

## 6.2 Helix geometry

First, a case of a curve with $C_H \neq 0$ and $C_V = 0$ is considered. If the vertical development angle $\theta$ is assumed constant, the curvature and torsion of the curve are defined, respectively, as

$$\kappa = \left| C_H \cos^2 \theta \right|, \qquad \tau = (1/2) C_H \sin 2\theta. \tag{15}$$

A curve can be both vertically elevated and twisted, but not super-elevated. This fact can be demonstrated by a helix curve. Recall that a circular helix $\mathbf{r}(s)$, as the one shown in Fig. 1a, is defined by the following equation:

$$\mathbf{r}(s) = \begin{bmatrix} x(s) \\ y(s) \\ z(s) \end{bmatrix} = \begin{bmatrix} a \cos \alpha \\ a \sin \alpha \\ b\alpha \end{bmatrix} \tag{16}$$

where $\alpha = s / \sqrt{a^2 + b^2}$, $s$ is the arc length parameter, $a$ is the helix radius, and $b/a$ is the slope of the helix. One can show that the curvature $\kappa$ and torsion $\tau$ are constant and defined as

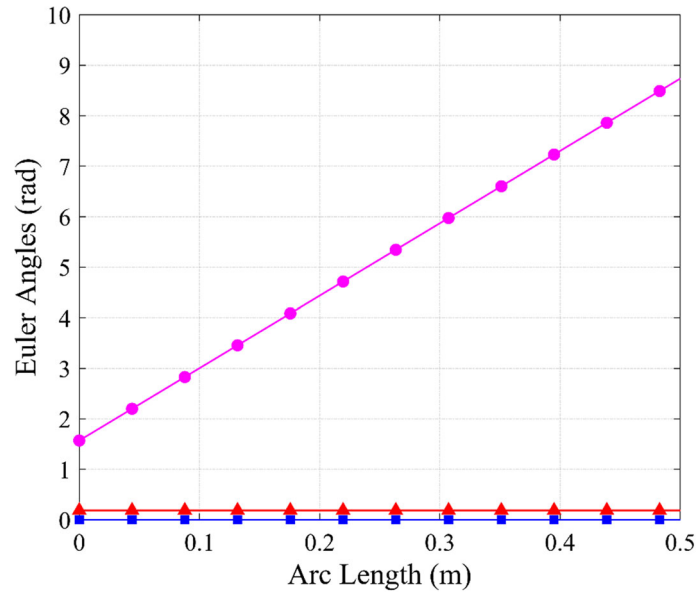$$\kappa = |a| / (a^2 + b^2), \qquad \tau = b / (a^2 + b^2). \tag{17}$$

**Fig. 2** Euler angles in the case of the helix curve (——■—— Euler angle $\phi = 0$ rad, ——▲—— Euler angle $\theta = 0.1849$ rad, ——●—— Euler angle $\psi$)

Using these equations, one can write $C_H$ and $\theta$ in terms of $a$ and $b$, respectively, as $C_H = \pm 1/a$ and $\tan \theta = \pm b/a$. In this case, the curve is not a planar curve, yet $C_V = 0$, and $\phi = 0$. That is, in the case of a helix with constant curvature and torsion, the vertical development angle $\theta$ is constant, and the Frenet bank angle $\phi$ is zero despite the fact that the curve is twisted. If the helix is projected on the horizontal plane, one has a circle of radius $a$ as shown in Fig. 1b, while a projection on the vertical plane leads to the geometric shape shown in Fig. 1c. Figure 2 shows the Euler angle solution of the differential equations of Eq. (5) in the case of the helix curve. The results presented in this Figure show nonzero horizontal curvature angle $\psi$, constant vertical elevation angle $\theta$, and a zero bank angle $\phi$. These results were obtained using the constants $a = 0.0686$ m, and $b = 0.01273$ m.

### 6.3 Explanation

The fact that the Frenet bank angle $\phi$ is equal to zero in the case of the helix curve can further be explained by evaluating the unit tangent vector $\partial \mathbf{r}/\partial s = (1/r)\begin{bmatrix} -a \sin(s/r) & a \cos(s/r) & b \end{bmatrix}^T$, where $r = \sqrt{a^2 + b^2}$. Using this tangent vector, the curvature vector, which defines the unit normal to the curve, is evaluated as $\partial^2 \mathbf{r}/\partial s^2 = -(a/r^2)\begin{bmatrix} \cos(s/r) & \sin(s/r) & 0 \end{bmatrix}^T$, which shows that the curvature vector has no vertical component. One can also show that if a particle is tracing the helix curve with a constant forward velocity $\dot{s}$, the particle acceleration $\mathbf{a}$ is given by $\mathbf{a} = -(a/r^2)\dot{s}^2\begin{bmatrix} \cos(s/r) & \sin(s/r) & 0 \end{bmatrix}^T$, which shows that the acceleration vector of the particle is in the horizontal plane and has no component along the vertical axis. That is, the particle has no gravity force component that balances its centrifugal force because of the zero Frenet bank angle $\phi$.

## 7 Spiral geometry and degree of continuity

The track spiral segment is used to connect two track segments with different geometric properties. The goal from using the spiral segment is to avoid abrupt geometric changes that can lead to jump discontinuities in the velocities and forces. Track spirals are designed to have linearly varying curvature. A spiral that connects a tangent segment to a curve segment has zero curvature at the point of intersection with the tangent segment and a nonzero curvature equal to that of the curve at the point of intersection with the curve. Within the spiral, the curvature varies linearly, and therefore, having the values of the horizontal curvature at the two endpoints $S_0$

and $S_1$, allows writing the horizontal curvature within the segment as $C_H(S) = (1 - \xi_c)C_H(S_0) - \xi_c C_H(S_1)$, where $\xi_c = S/(S_1 - S_0)$. This equation can be used to define the horizontal curvature angle $\psi$ as previously discussed in this paper. It is important to point out that continuity of the horizontal curvature does not ensure continuity of Euler angles or the gradients (slopes). For example, two curve segments can have the same curvature at an intersection point, but still have a cusp discontinuity at this intersection point. At this point, the tangents (gradients or slopes) are not the same; that is, the curve is continuous but not smooth. Furthermore, a curve segment may not be twisted, but it can be super-elevated to achieve a certain balance speed, that is, $C_H^c \neq 0$ and $\phi^c \neq 0$, where superscript $c$ refers to the curve segment. The constant curve segment has zero vertical curvature and zero vertical development angle, that is, $C_V^c = 0$ and $\theta^c = 0$. This super-elevated curve can be connected to a spiral segment whose other end is connected to a tangent segment which has zero horizontal curvature.

### 7.1 Transition points

As demonstrated by the helix example, a curve can be vertically elevated and twisted, while the Frenet bank angle $\phi$ is equal to zero. A spiral segment connecting tangent and super-elevated curve segments can be vertically elevated and twisted, demonstrating the need for proper interpretation of the angle representation. In this case, the vertical curvature, the vertical development angle, and the horizontal curvature are not zero, that is, $C_V^s \neq 0$, $\theta^s \neq 0$, and $C_H^s \neq 0$, where superscript $s$ refers to the spiral segment. This example shows that the spiral and curve at the intersection point have different values for the Frenet bank angle. Because the tangent and curve segments have simple geometry that does not require numerical integration, one must use consistent data at the intersection points in order to ensure accurate numerical construction of the spiral geometry. This can be further made clear from the simple example discussed in the following Section which demonstrates non-uniqueness of the values of the angles at the transition points.

### 7.2 ANCF curve and gradient continuity

In the preprocessor computer program that produces the track data file, the continuity of the horizontal curvature $C_H$ is used with other conditions to determine Euler angles and the global positions of the track nodal points. During the dynamic simulations, the position and the angle coordinates are used to determine the locations of the wheel/rail contact points within a track segment. This representation ensures continuity of the tangent vectors at the nodes when the *absolute nodal coordinate formulation* (ANCF) finite elements are used as the basis for the interpolation [18, 30]. Nonetheless, curvature continuity is not normally enforced during the dynamic simulations despite the fact that the principal curvatures and principal directions at the contact points are evaluated in order to be able to compute the dimensions of the contact ellipse using Hertz's contact theory [31, 32].

## 8 Discontinuity and track data

In this Section a simple track model is used to discuss the discontinuity and the problems that arise if distinction is not made between the Frenet bank angle $\phi$ and the track bank angle $\phi_t$. based on the equations obtained in this paper. The track model used as an example in this Section has a tangent and curved segments connected by a spiral. The curved segment is super-elevated as it is often the case in practice.

**Table 1** Preprocessor track data

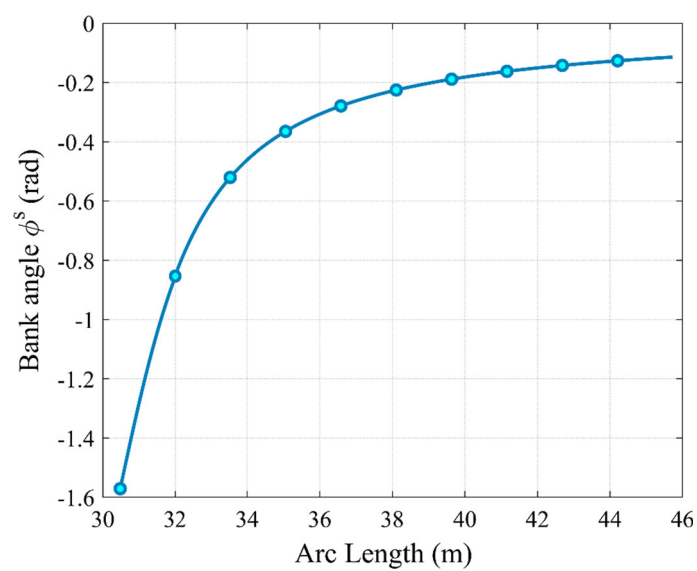| Arc length (m) | Horizontal curvature (m$^{-1}$) | Super-elevation (m) | Vertical development angle $\theta$ (rad) |
| --- | --- | --- | --- |
| $s_0 = 0.0$ | 0 | 0 | 0 |
| $s_1 = 30.48$ | 0 | 0 | 0 |
| $s_2 = 45.72$ | 0.00286 | 0.0381 | 0.005 |

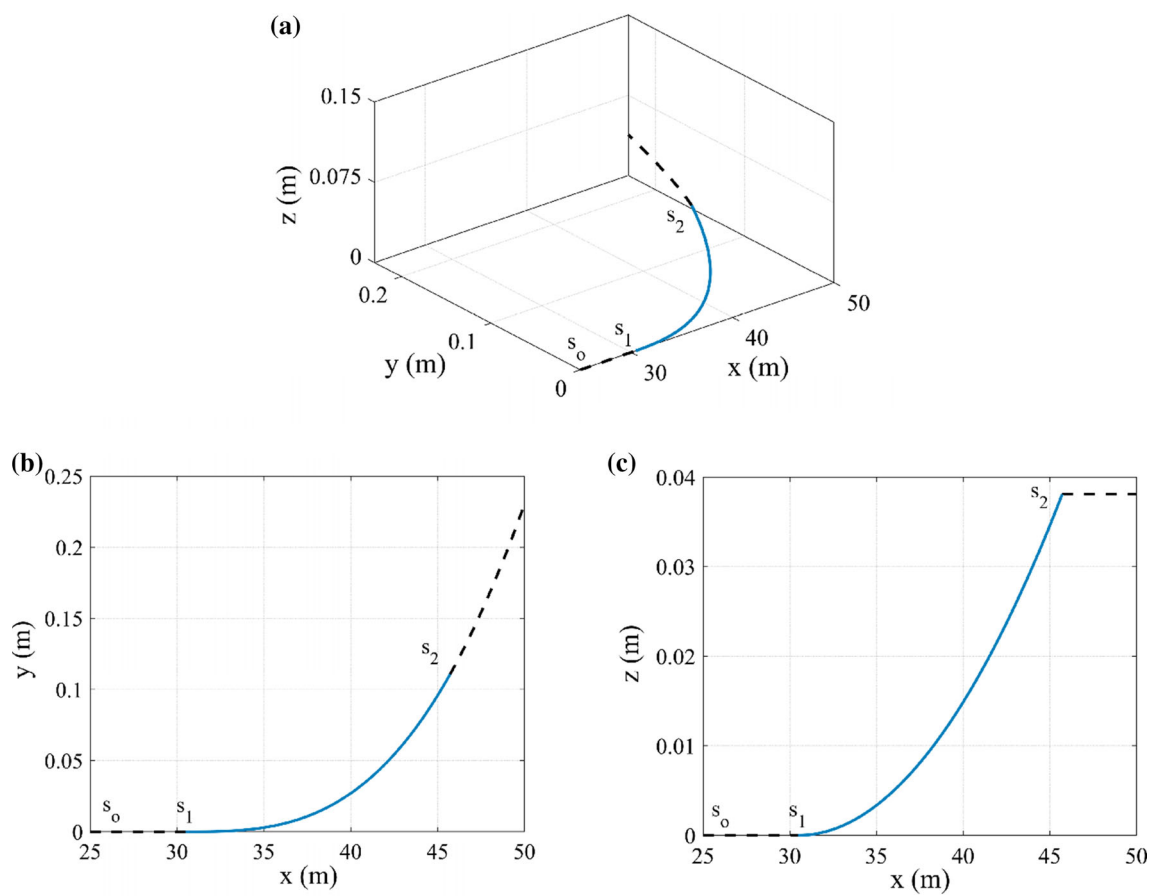**Fig. 3** Frenet Bank angle within the spiral segment



**Fig. 4** Spiral geometry with continuity of the horizontal curvature

### 8.1 Track model and results

Typical railroad curved-track data used as input to the preprocessor computer program that produces the numerical representation of the track geometry are shown in Table 1. The data in this Table describe the input parameters for defining a curved track that consists of tangent and spiral segments. The start point of the tangent segment is at the origin defined by the arc length parameter value $s_0 = 0$ m, while the endpoints of the spiral are defined by the values of $s_1$ and $s_2$ provided in Table 1. The geometric properties at the start point of the spiral segment are of zero values, while at the endpoint, $C_H = 0.00286$ m$^{-1}$ and $\theta = 0.005$ rad. The horizontal and vertical curvatures within the spiral segment can be defined by using the method described in this paper. Using the data presented in Table 1, Eq. (14) can be solved for the angles within the spiral segment. The solution of the Frenet bank angle $\phi$ along the segment is shown in Fig. 3. Using the solution of Eq. (14), the geometry of the spiral segment can be fully determined as shown in Fig. 4. It is clear from the results presented in Fig. 4 that the track curve is not smooth at the transition from the spiral to the curve. This is despite the fact that continuity is imposed on the horizontal curvature.

### 8.2 Gradient continuity

Another alternate approach can be used to define the spiral geometry by using the ANCF cable element [18, 30]. In this case, the position and gradient coordinates at the two endpoints of the spiral are used with the ANCF cubic interpolation instead of using the procedure described in this paper. Using ANCF finite elements, continuity can be imposed on the position gradients ensuring smoothness at the transition points. The displacement field of the ANCF cable element can be written as $\mathbf{r}(x) = \mathbf{S}(x)\mathbf{e}$, where $\mathbf{r}$ is the global position vector on the track
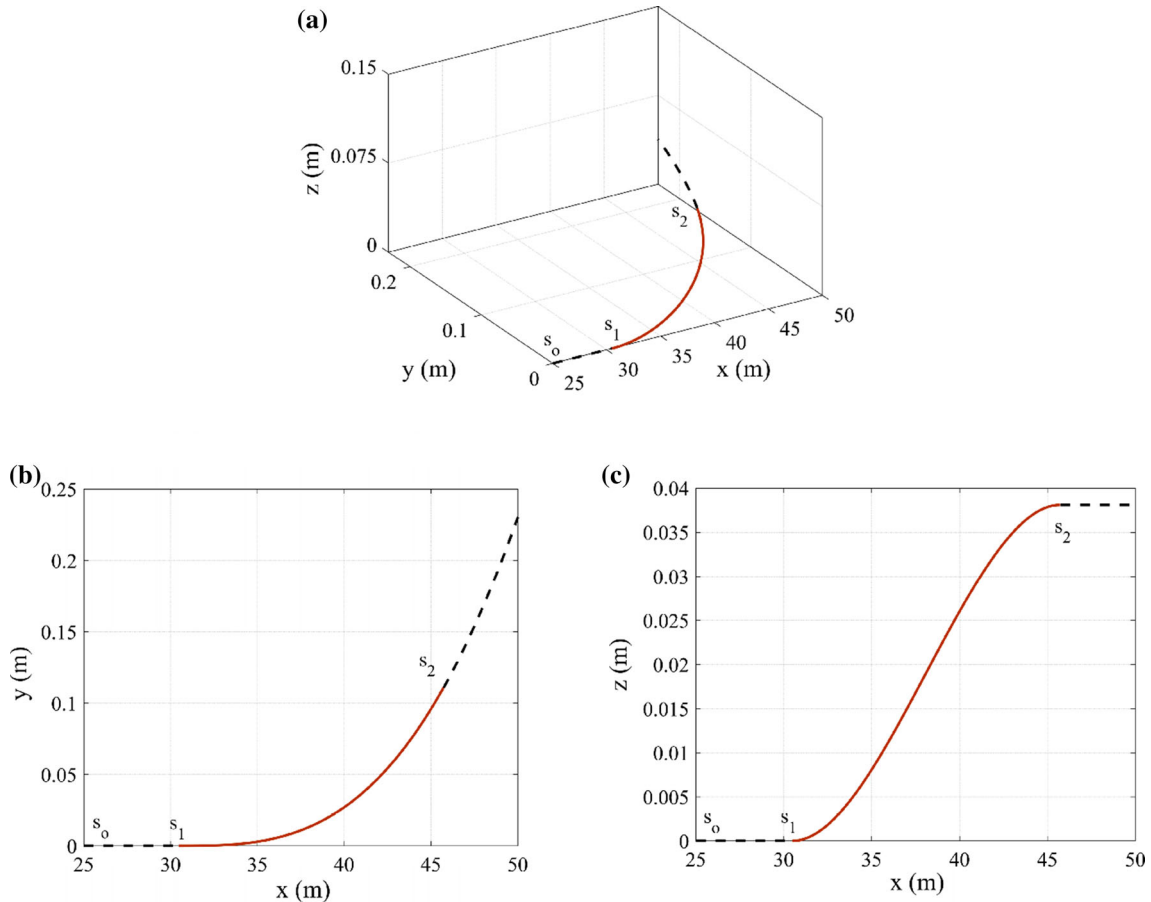


**Fig. 5** ANCF spiral segment

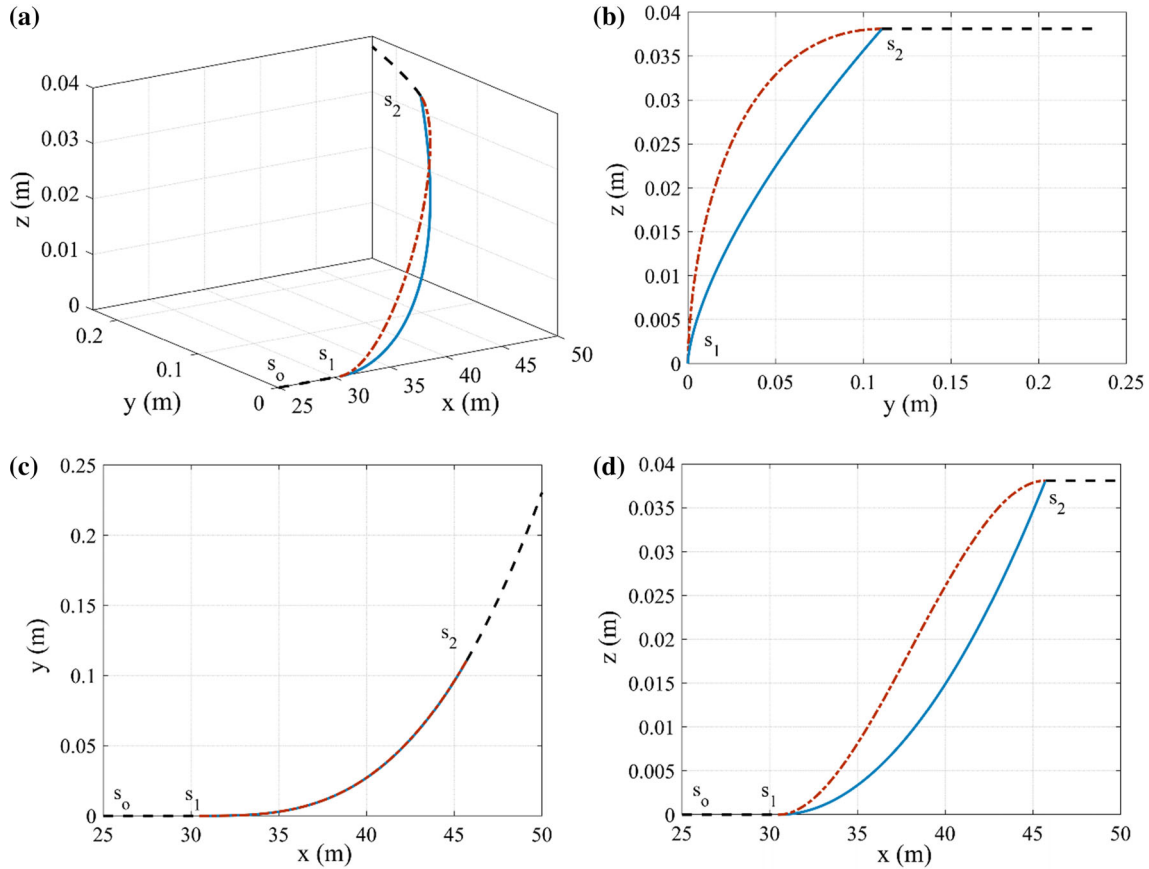**(a)**



**(b)**



**(c)**



**(d)**



**Fig. 6** Comparison between the geometry of a spiral segment with ANCF cubic curve and linearly interpolated horizontal curvature curve (— · — · — ANCF curve, ——— linearly interpolated horizontal curvature)

segment, $\mathbf{S}$ is the element shape function matrix, $\mathbf{e}$ is the vector of the element nodal coordinates, and $x$ is the element spatial coordinate [30]. The cable element has two nodes, and the vector of nodal coordinates at each node consists of its position and gradient vector; that is, $\mathbf{e}^k = \left[ \mathbf{r}^{k^T} \ \mathbf{r}_x^{k^T} \right]^T$, where superscript $k$, $k = 1, 2$, refers to the node number, and $\mathbf{r}_x = \partial \mathbf{r} / \partial x$ is the position gradient vector. Imposing continuity of the position gradient vector at the endpoints achieves smoothness but does not ensure curvature continuity. By using the ANCF cable element position and gradient coordinates to define the geometry, one obtains the geometric representation shown in Fig. 5. A comparison between the curve geometry obtained using the procedure used in railroad practice, described in detail in this paper, and the ANCF geometry is shown in Fig. 6. It is clear from the results presented in Figs. 5 and 6 that smoothness is achieved by imposing the gradient continuity. It is important, however, to point out that when the ANCF element is used, no assumption is made that the curvature varies linearly within the element. While a cubic interpolation in $x$ is used for this element and $\partial \mathbf{r}^2 / \partial x^2$ is linear in $x$, an accurate definition of the curvature using the arc length parameter $s$ demonstrates that the curvature is not a linear function of the arc length [30]. The results presented in Fig. 6 demonstrate the degree of smoothness achieved by imposing the gradient continuity using the ANCF element. The curve with the curvature continuity, on the other hand, is not smooth at the spiral/curve transition.

## 8.3 Discontinuity

Equation (10), $\phi = \tan^{-1}\left(-C_V / C_H \cos^2 \theta\right)$, which defines the Frenet bank angle, is an algebraic equation. If the desired super-elevation at the endpoint of the spiral intersection with a super-elevated curve is provided, one can obtain the corresponding value of the development angle $\theta_2^s$ at this spiral/curve intersection point. The value of $C_V$ can then be determined and used in Eq. (14) to define the bank angle at this transition point. For the
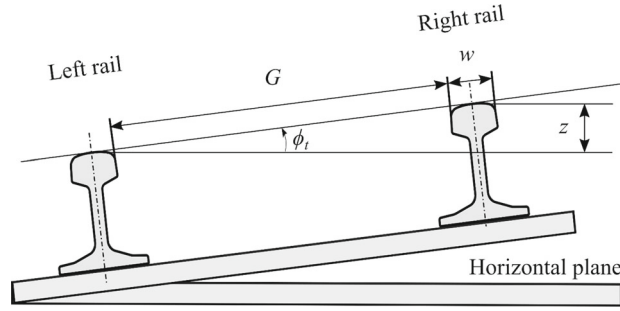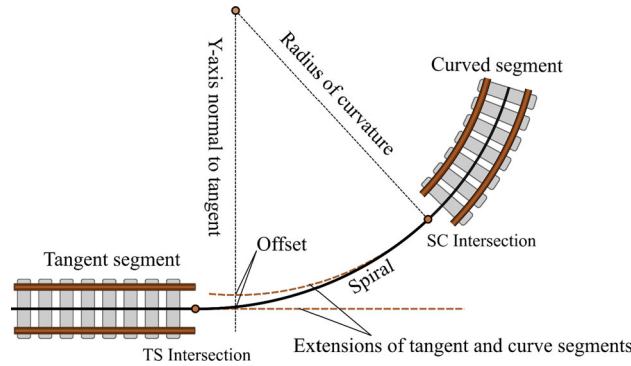
**Fig. 7** Track super-elevation



**Fig. 8** Offset definition (TS is tangent/spiral, SC is spiral/curve) [33]

example considered in this Section, the curve segment is super-elevated by the bank angle $\phi_t^c = 0.0268$ rad, which also defines the super-elevation at the spiral endpoint. Because at the tangent/spiral intersection all Euler angles are zero and for the spiral segment $\triangle s = s_2 - s_1 = 15.24$ m, the constant value of the vertical curvature can be written as $C_V = (\theta_2 - \theta_1)/(s_2 - s_1) = \theta_2/15.24$. Because the super-elevated curve segment has zero grade in the simple example considered in this Section, the position $z$-coordinate at the spiral/curve intersection is determined from the curve segment super-elevation resulting from the rotation of the curve about the left (lower) rail, as shown in Fig. 7. The vertical position of the super-elevated curve segment can be obtained using the equation $z = G \sin \phi_t$, where $G = 1.42$ m is the track gage. The integration of the curve unit tangent, which is the first column of the matrix of Eq. (1), determines the position of points along the track segments [18, 19]. For the spiral segment, one has $z(s) = (1 - \cos \theta(s))/C_V$, which upon defining $z$ with respect to the left rail (not track centerline), leads to $0.0025 = (1 - \cos \theta_2)/\theta_2$. This nonlinear equation can be solved to determine $\theta_2 = 0.005$ rad and the corresponding vertical curvature $C_V = 3.2808 \times 10^{-4}$ m$^{-1}$.

## 9 Comparison with previous approaches

In this Section, the basic differences between the approach presented in this paper for the description of the spiral geometry and the approach used by Klauder [33] are discussed. This Section also presents some practical considerations that need to be considered when super-elevating the track.

In the approach used by Klauder, the curvatures at two spiral ends are used to develop the linear expression of the curvature based on a tentative spiral length. The direction of the longitudinal tangent on the horizontal plane at each point on the spiral curve can be defined in terms of the horizontal plane $x$ and $y$ coordinates using Fresnel integrals (see the Appendix). After the coordinates of the spiral two endpoints are determined, an offset is determined by extending the tangent and curve segments as shown in Fig. 8. The value of the obtained offset has to be compared with a given value if there is any, and the spiral length is adjusted iteratively until the obtained offset satisfies the requirement.

In the steps summarized by Klauder for the track layout, it is assumed that the spiral geometry is represented by a planar curve without considering the grade. Consequently, the curvature referred to above is considered as the horizontal curvature. The bank angle $\phi$ is obtained by solving the balancing equation

$\mathrm{d}\psi\big/\mathrm{d}s = \big(g\big/(v_d)^2\big)\tan\phi(s)$ along the segment, where $g$ is the gravity constant, and $v_d$ is the balance speed of the curve. Due to the small angle assumption used in practice, the bank angle is assumed to be proportional to the track curvature, where the difference between $\phi$ and $\tan\phi$ does not exceed 0.5%. In the case of a spiral, where the curvature is linearly interpolated as function of the arc length, the bank angle is assumed to be subject to the same linearity assumption. The track super-elevation is then achieved by raising the to-be high rail by ensuring that the track plane has the appropriate bank angle.

The concept of the offset, as the minimum distance between extensions of the segments that maintain their respective fixed curvatures, is introduced in the procedure for determining the spiral geometry. As discussed in the literature, a longer spiral with a lower rate of curvature variation leads to larger offset. While a shorter spiral segment has been preferred in the past because of the manufacturing, assembly, and maintenance cost, a relatively short spiral can result in a smaller offset and track warpage. For this reason, the offset requirement needs to be considered in order to adjust the spiral length such that the track warpage is avoided.

While the practical considerations highlighted above need to be taken into account in the actual track layout, it is important to mention some fundamental geometric differences between the approach used by Klauder [33] and the approach discussed in this paper. First, when considering the curve geometry, Klauder assumes linear interpolation of the track bank angle $\phi_t$, an assumption that implies that this angle within the segment is independent of the curvature and vertical elevation angles and no distinction is made between $\phi$ and $\phi_t$. Second, in this paper, the gravity constant is not used in the geometric description of the spiral. Third, an iterative procedure is used by Klauder to determine the length of the spiral segment in order to satisfy certain offset value requirements. This offset issue is not addressed in this paper.

## 10 Summary and conclusions

In the design of the rail track, geometry plays a central role and directly influences the quality of the computer simulation results. Based on given inputs, the geometry of the track space curve can be constructed and numerically represented using a large number of nodal points. The geometry of a space curve can be completely defined in terms of two parameters: the *horizontal* and *vertical curvatures*, or equivalently, the curve curvature and torsion; this is with the understanding that zero vertical curvature does not imply zero torsion, as discussed in this paper and demonstrated by the helix curve example. In the case of zero vertical curvature, the torsion can be nonzero if the vertical development angle is nonzero, as it is the case with the helix curve example. In railroad vehicle systems, the *track bank angle* is associated with the track *super-elevation* required to achieve a certain *balance speed* required for the safe operation of the vehicle. In practice, Euler angles are often used in the formulation of the track space-curve differential equations. Using this approach, however, one can show, as demonstrated in this paper, the dependence of the Frenet bank angle on two independent parameters, often used as inputs in the definition of the track geometry. The general differential equations that govern the track geometry using the Euler angle sequence adopted by the rail industry are developed. The paper demonstrates that the Frenet bank angle can be determined from two other independent variables, and consequently, a distinction must be made between the Frenet bank angle $\phi$ and the track bank angle $\phi_t$ used to define the orientation frames that follow the vehicle components in railroad vehicle algorithms.

Using the helix curve example, the paper demonstrates that a curve can be twisted and vertically elevated, but not super-elevated. It is shown that the helix curvature vector, which is along the unit normal to the curve, remains in the horizontal plane, and the acceleration of a particle tracing the helix curve with a constant forward velocity has no vertical component. This result, which is consistent with the fact that a helix has zero Frenet bank angle, demonstrates that the particle has no gravity force component that balances the centrifugal force. The paper also discusses the continuity conditions at the track segment transitions. As explained in the paper, imposing curvature continuity does not ensure continuity of the tangent vectors at the curve/spiral intersection. An ANCF finite element is used to develop the spiral geometry by imposing gradient continuity instead of curvature continuity. The geometry results obtained using the ANCF element are compared with the geometry results obtained using the curvature continuity.

## Appendix

### Fresnel integrals

The Fresnel integrals $S(x)$ and $C(x)$ are defined by following power-series expansions which converge for all values of the argument $x$:

$$\left.\begin{array}{l} S(x) = \int_0^x \sin(t^2)\,\mathrm{d}t = \sum_{n=0}^{\infty} (-1)^n \frac{x^{4n+3}}{(2n+1)!(4n+3)} \\ C(x) = \int_0^x \cos(t^2)\,\mathrm{d}t = \sum_{n=0}^{\infty} (-1)^n \frac{x^{4n+1}}{(2n)!(4n+1)} \end{array}\right\}. \tag{18}$$

The trace of the parametric plot of Fresnel integrals $[C(x), S(x)]$ is called an *Euler spiral* or a *clothoid*, whose curvature at any point is proportional to the distance from the origin.

## References

1. Pascal, J.P., Sany, J.R.: Dynamics of an isolated railway wheelset with conformal wheel–rail interactions. Veh. Syst. Dyn. **54**, 1947–1969 (2019)
2. Zhang, Y., El-Sibaie, M., Lee, S.: FRA track quality indices and distribution characteristics. In: AREMA 2004 Annual Conference, Nashville, TN, USA (2004)
3. Andersson, C., Abrahamsson, T.: Simulation of interaction between a train in general motion and a track. Veh. System Dyn. **38**, 433–455 (2002)
4. True, H.: Does a critical speed for railroad vehicles exist? In: Proceedings of IEEE/ASME Joint Railroad Conference, pp. 125–131 (1994)
5. Berghuvud, A.: Freight car curving performance in braked conditions. IMechE J. Rail Rapid Transit **216**, 23–29 (2002)
6. Boocock, D.: The steady-state motion of railway vehicles on curved track. J. Mech. Eng. Sci. **2** (1969)
7. De Pater, A.D.: The geometrical contact between track and wheel-set. Veh. Syst. Dyn. **17**, 127–140 (1988)
8. Elkins, J.A., Gostling, R.J.: A general quasi-static curving theory for railway vehicles. In: Proceedings of 2nd IUTAM Symposium, Vienna, pp. 388–406 (1977)
9. Endlicher, K.O., Lugner, P.: Computer simulation of the dynamical curving behavior of a railway bogie. Veh. Syst. Dyn. **19**, 71–95 (1990)
10. Gilchrist, A.O.: The long road to solution of the railway hunting and curving problems. IMechE J. Rail Rapid Transit **212**, 219–226 (1998)
11. Grassie, S.L.: Dynamic modeling of the track. In: Kalker, J.J., Cannon, D., Orringer, O. (eds.) Rail quality and maintenance for modern railway operation. Kluwer, Dordrecht (1993)
12. Hamid, A., Rasmussen, K., Baluja, M., Yang, T-L.: Analytical description of track geometry variations. FRA report no. DOT/FRA/ORD-83/03.1 (1983)
13. Handoko, Y., Xia, F., Dhanasekar, M.: Effect of asymmetric brake shoe force application on wagon curving performance. Veh. Syst. Dyn. Suppl. **41**, 113–122 (2004)
14. Kerr, A.D., El-Sibaie, M.A.: On the new equations for the lateral dynamics of rail-tie structure. ASME J. Dyn. Syst. Meas. Control **107**, 180–185 (1987)
15. Kik, W.: Comparison of the behavior of different wheelset-track models. Veh. Syst. Dyn. **20**, 325–339 (1992)
16. Knothe, K.L., Grassie, S.L.: Modeling of railway track and vehicle/track interaction at high frequencies. Veh. Syst. Dyn. **22**, 209–262 (1993)
17. Knothe, K., Stichel, S.: Direct covariance analysis for the calculation of creepages and creep-forces for various bogie on straight track with random irregularities. Veh. Syst. Dyn. **23**, 237–251 (1994)
18. Shabana, A.A., 2021, *Mathematical Foundation of Railroad Vehicle Systems*, Wiley & Sons (in press)
19. Shabana, A.A., Zaazaa, K.E., Sugiyama, H.: Railroad Vehicle Dynamics: A Computational Approach. CRC Press, Boca Raton (2008)
20. Wickens, A.: Fundamentals of Rail Vehicle Dynamics. CRC Press, Boca Raton (2005)
21. Rathod, C., Shabana, A.A.: Geometry and differentiability requirements in multibody railroad vehicle dynamic formulations. Nonlinear Dyn. **47**(1–3), 249–261 (2007)
22. Shabana, A.A., Ling, H.: Noncommutativity of finite rotations and definitions of curvature and torsion. ASME J. Comput. Nonlinear Dyn. **14**(9) (2019)
23. Kreyszig, E.: Differential Geometry. Dover Publications, New York (1991)
24. Do Carmo, M.P.: Differential Geometry of Curves and Surfaces. Prentice Hall, Englewood Cliffs (1976)
25. Klauder Jr., L.T., Chrismer, S.M., Elkins, J.: Improved spiral geometry for high-speed rail and predicted vehicle response. Transp. Res. Rec. **1785**(1), 41–49 (2002)
26. Levent, A., Sahin, B., Habib, Z.: Spiral Transitions. Appl. Math. J. Chin. Univ. **33**, 468–490 (2018)
27. Hedrick, J.K., Arslan, A.V.: Nonlinear analysis of rail vehicle forced lateral response and stability. ASME J. Dyn. Syst. Meas. Control **101**, 230–237 (1979)
28. Jeambey, J.: Improving high speed stability of freight cars with hydraulic dampers. In: Proceedings of the 1998 ASME International Mechanical Engineering Congress & Exposition (Rail Transportation), Anaheim, California (1998)

29. Matsumoto, A., Sato, A., Ohno, Y., Suda, H., Nishimura, Y., Tanimoto, R., Oka, M.: Compatibility of curving performance and hunting stability of railway bogie. Veh. Syst. Dyn. Suppl. **33**, 740–748 (1999)
30. Shabana, A.A.: Computational Continuum Mechanics, 3rd edn. Wiley, London (2018)
31. Johnson, K.L.: Contact Mechanics. Cambridge University Press, Cambridge (1985)
32. Kalker, J.J.: Three-Dimensional Elastic Bodies in Rolling Contact. Kluwer, Dordrecht (1990)
33. Klauder, L.T.: Railroad spiral design and performance. In: Proceedings of the 2012 Joint Rail Conference, American Society of Mechanical Engineers Digital Collection, pp. 9–21 (2012)